Richter, MJ, Wagmann, L, Brandt, SD and Meyer, MR

In vitro metabolic fate of the synthetic cannabinoid receptor agonists 2F-QMPSB and SGT-233 including isozyme mapping and carboxylesterases activity testing

Journal of Analytical Toxicology – accepted

In Vitro Metabolic Fate of the Synthetic Cannabinoid Receptor Agonists 2F-QMPSB and SGT-233 Including Isozyme Mapping and Carboxylesterases Activity Testing

Matthias J. Richter[1], Lea Wagmann[1], Simon D. Brandt[2], Markus R. Meyer[*1]

[*] Author to whom correspondence should be addressed. Markus R. Meyer, Department of Experimental and Clinical Toxicology, Institute of Experimental and Clinical Pharmacology and Toxicology, Center for Molecular Signaling (PZMS), Saarland University, 66421 Homburg, Germany, markus.meyer@uks.eu

[1]Department of Experimental and Clinical Toxicology, Institute of Experimental and Clinical Pharmacology and Toxicology, Center for Molecular Signaling (PZMS), Saarland University, Homburg, Germany

[2]School of Pharmacy and Biomolecular Sciences, Liverpool John Moores University, Liverpool, UK

Abstract

2F-QMPSB (quinolin-8-yl 3-(4,4-difluoropiperidine-1-sulfonyl)-4-methylbenzoate) and SGT-233 (3-(4,4-difluoropiperidine-1-sulfonyl)-4-methyl-*N*-(2-phenylpropan-2-yl)benzamide) belong to a new group of synthetic cannabinoid receptor agonists (SCRAs) containing a sulfamoyl benzoate or sulfamoyl benzamide core structure. 2F-QMPSB was identified on herbal material seized in Europe in 2018. The aims of the presented study were the identification of in vitro phase I and II metabolites of 2F-QMPSB and SGT-233 to find analytical targets for toxicological screenings. Furthermore, the contribution of different monooxygenases and human carboxylesterases to phase I metabolism was investigated. Liquid chromatography coupled to high-resolution tandem mass spectrometry was used for analysis. Ester hydrolysis was found to be an important step in the metabolism of 2F-QMPSB, which was catalyzed mainly by hCES1 isoforms. Additionally, non-enzymatic ester hydrolysis was observed in case of 2F-QMPSB. Notably, the carboxylic acid product derived from ester hydrolysis and metabolites thereof were only detectable in negative ionization mode. In case of SGT-233, mono- and dihydroxy metabolites were identified, as well as glucuronides. CYP2C8, CYP2C9, CYP2C19, CYP3A4, and CYP3A5 were found to be involved in the hydroxylation of both compounds. The results of these in vitro experiments suggest that the ester hydrolysis products of 2F-QMPSB and their glucuronides are suitable targets for toxicological screenings. In the case of SGT-233, the mono- and dihydroxy metabolites were identified as suitable screening targets. The involvement of various CYP isoforms in the metabolism of both substances reduces the likelihood of drug-drug interactions due to CYP inhibition.

Keywords: new psychoactive substances; synthetic cannabinoid receptor agonists; pooled human liver S9 fraction; LC-HRMS/MS; isozyme mapping; carboxylesterases activity testing

Introduction

The emergence of new psychoactive substances (NPS) continues to be a major concern for public health (1, 2). In addition to stimulants and synthetic opioids, synthetic cannabinoids, also known as synthetic cannabinoid receptor agonists (SCRAs), represent a large group of NPS (1). Constant modification of chemical structures aims to circumvent legislation and introduces further NPS into the drug market (3). Although the number of newly detected NPS in the EU has decreased in recent years, SCRAs continue to represent an important proportion (3). SCRAs are often being sprayed on plant material and sold on the drug market, for example in the form of 'herbal smoking mixtures' (3).

In 2007, a high throughput screening identified QMPSB (quinolin-8-yl 4-methyl-3-(piperidine-1-sulfonyl)benzoate) (Figure S1 in the Electronic Supplementary Material, ESM) as a potent SCRA (4). QMPSB was reported to be a full agonist at the cannabinoid receptors CB1 and CB2 with moderate selectivity for the CB2 receptor (4, 5). Therefore, QMPSB became a template for a series of other SCRAs based on a sulfamoyl benzoate or sulfamoyl benzamide core structure and/or a quinolin-8-yl ester head group. In 2012, a company began to research this new SCRA group. To increase the potency of QMPSB, 4,4-difluoropiperidine was introduced resulting in the compound quinolin-8-yl 3-(4,4-difluoropiperidine-1-sulfonyl)-4-methylbenzoate (2F-QMPSB, also known as QMDFPSB and SGT-13). Investigations with human volunteers showed a higher potency of 2F-QMPSB compared to QMPSB. In addition, 2F-QMPSB provided better temperature stability and solubility than QMPSB (6). In 2018, 2F-QMPSB appeared as an NPS in Europe. It was detected on plant material contained in a seized postal shipment in Italy (7). The substances PB-22 (QUPIC) and BB-22 (QUCHIC) are other examples of similar SCRAs which appeared on the NPS market, created by combining the quinolin-8-yl ester head group with an *N*-alkyl-1*H*-indole core (8). In further investigations of this SCRA group, the head group of 2F-QMPSB was converted into a

cumylamide, which is present in potent SCRAs such as CUMYL-PINACA (9). This led to the compound SGT-233 (3-(4,4-difluoropiperidine-1-sulfonyl)-4-methyl-*N*-(2-phenylpropan-2-yl)benzamide) (Figure S1). However, SGT-233 showed lower potency than QMPSB (6). This is in agreement with a previous study, in which the sulfamoyl benzamide SCRAs showed a lower potency than their sulfamoyl benzoates (4).

Data on the metabolism of emerging NPS are important in clinical and forensic toxicology to develop screening methods for plasma or urine samples. For most SCRAs, only metabolites are detectable in urine, thus knowledge of excreted metabolites is crucial (10). To our knowledge, no data on the metabolism of 2F-QMPSB and SGT-233 are available in literature. Therefore, the aim of the study was the identification of metabolites of both SCRAs as potential targets for toxicological screening approaches by liquid chromatography coupled to high-resolution tandem mass spectrometry (LC-HRMS/MS). Phase I and II metabolites should be identified using in vitro incubations with pooled human liver S9 fraction (pHLS9). An in vitro monooxygenases activity screening should be performed to investigate the involvement of individual monooxygenases in phase I metabolism. A carboxylesterases activity assay should be done for 2F-QMPSB, to demonstrate enzyme-catalyzed cleavage, as the chemical instability of the ester linker had already been observed in a previous study with QMPSB (11).

Materials and Methods

Chemicals and reagents

2F-QMPSB and SGT-233 were made available by Stargate International (Auckland, New Zealand) (6). Stock solutions of 2F-QMPSB and SGT-233 were prepared in acetonitrile (1 mg/mL) and stored at -18°C. Trimipramine-d3 and glibenclamide were purchased from LGC

Standards (Wesel, Germany). Isocitrate, isocitrate dehydrogenase, superoxide dismutase, 3′-phosphoadenosine-5′-phosphosulfate (PAPS), S-(5′-adenosyl)-L-methionine (SAM), dithiothreitol, reduced glutathione, acetyl coenzyme A, magnesium chloride ($MgCl_2$), potassium dihydrogen phosphate (KH_2PO_4), dipotassium hydrogen phosphate (K_2HPO_4), and tris hydrochloride were purchased from Sigma-Aldrich (Taufkirchen, Germany). $NADP^+$ was bought from Biomol (Hamburg, Germany). Baculovirus-infected insect cell microsomes (Supersomes) containing the human cDNA-expressed cytochrome P450 isozymes CYP1A2 (1 nmol/mL), CYP2A6 (2 nmol/mL), CYP2B6 (1 nmol/mL), CYP2C8 (1 nmol/mL), CYP2C9 (2 nmol/mL), CYP2C19 (1 nmol/mL), CYP2D6 (1 nmol/mL), CYP2E1 (2 nmol/mL), CYP3A4 (1 nmol/mL), CYP3A5 (1 nmol/mL), or flavin-containing monooxygenase 3 (FMO3, 5 mg/mL), as well as pooled human liver microsomes (pHLM, 20 mg protein/mL, 360 pmol total CYP/mg, 26 donors), pHLS9 (20 mg protein/mL, 8 donors), recombinant human carboxylesterase hCES1b (5 mg/mL), hCES1c (5 mg/mL), hCES2 (5 mg/mL), UGT reaction mixture solution A (25 mM UDP-glucuronic acid), and UGT reaction mixture solution B (250 mM Tris HCl, 40 mM $MgCl_2$, and 125 µg alamethicin/mL) were purchased from Corning (Amsterdam, The Netherlands). After delivery, the enzymes were thawed at 37°C, aliquoted, snap-frozen in liquid nitrogen, and stored at -80°C until use. Acetonitrile (LC-MS grade), methanol (LC-MS grade), ammonium formate (analytical grade), formic acid (LC-MS grade), and all other reagents and chemicals (analytical grade) were obtained from VWR (Darmstadt, Germany).

pHLS9 incubations for investigation of phase I and II metabolites

2F-QMPSB and SGT-233 were incubated with pHLS9 according to an earlier publication with minor modifications (12): In comparison, the AcCoA system was omitted as acetylation was not expected to be a main metabolic pathway for the substances investigated. The final

solutions were incubated for 6 hours, with a 60µL sample taken after 1 hour. 2.5µM Trimipramine-d3 was used as an internal standard (IS).

Monooxygenases activity screening

2F-QMPSB and SGT-233 were incubated with recombinant monooxygenases as described in a previous study with minor modifications (13). In comparison, trimipramine-d3 was used at a lower concentration of 2.5µM as an internal standard and the samples were centrifuged at 18.407 x g for 2min after the incubation period.

Carboxylesterases activity screening

Incubations with human carboxylesterases were conducted as described in a previous publication with minor modifications (14). 2F-QMPSB (10 µM final concentration) was incubated in phosphate buffer 100 mM pH 7.4 containing hCES1b, hCES1c, hCES2 (5 ng/µL final concentration each), pHLM, or pHLS9 (50 ng/µL final concentration each) for 45 min at 37°C. The final incubation volume was 200 µL. The incubations were started by adding 2F-QMPSB. To evaluate non-enzymatic ester hydrolysis, negative control incubations (without enzyme) were conducted. At 0, 8, 14, 20, 30, and 45 min, 20 µL samples were taken. The reactions in these samples were stopped immediately with 60 µL ice-cold acetonitrile containing glibenclamide (5 µM) as IS. After centrifugation for 2 min at 18,407 x g, the supernatant was transferred to an autosampler vial and analyzed using LC-HRMS/MS. All incubations were performed in duplicates (n=2).

LC-HRMS/MS settings

For all experiments, a Thermo Fisher Scientific (TF, Dreieich, Germany) Dionex UltiMate 3000 RS LC system consisting of a degasser, a quaternary pump, and a HTC PAL autosampler (CTC Analytics AG, Zwingen, Switzerland) coupled to a TF Q-Exactive mass spectrometer with heated electrospray ionization (HESI)-II source was used. According to the manufacturer's recommendations, an external mass calibration was done before analysis. All samples were injected with a volume of 5 µL. In accordance with an earlier publication, a gradient elution was performed on a TF Accucore Phenyl-Hexyl column (100 mm x 2.1 mm, 2.6 µm) at 40°C (15). The HESI-II source settings were used, which were already described in a previous publication, whereby the samples were also measured in a separate run in the negative ionization mode in addition to the positive ionization mode (16). Mass spectrometer settings and subsequent data analysis were performed as described in a previous study, with the scan range for the expected metabolites set to *m/z* 80-850 (16).

Results and discussion

Identification of in vitro phase I and II metabolites of 2F-QMPSB

For the identification of phase I and II metabolites, exact protonated or deprotonated precursor ion (PI) masses of expected metabolites were calculated. High-resolution full scan data were examined for these exact PI masses. Corresponding MS^2 spectra were then interpreted. Deviations between measured and calculated PI mass were only tolerated up to 5 ppm. All metabolites were tentatively identified as no reference material was available for them.

A total of ten phase I and four phase II 2F-QMPSB metabolites were identified in pHLS9 and/or CYP isozyme incubations (metabolites QM1-QM14; Table S1). Table S1 (ESM)

contains the ionization mode (positive or negative) and the incubation type (pHLS9 and/or CYP isozyme incubation) in which the respective metabolite was detected.

Eight metabolites were identified in pHLS9 incubations. All metabolites were ester hydrolysis products or metabolites derived therefrom. No metabolite with an intact ester moiety could be detected in pHLS9 incubations. The two ester hydrolysis products QM5 and QM10 (Table S1) could also be detected in the negative control incubations. Since the negative control incubations do not contain any enzymes, rapid non-enzymatic ester hydrolysis must be assumed here. All metabolites identified in pHLS9 incubations were detected in the one hour samples as well as in the six hours samples.

The MS^2 spectra of 2F-QMPSB and its most abundant metabolite in pHLS9 incubations, the ester hydrolysis product QM5, are shown in Figure 1. The MS^2 spectra of further metabolites are given in Figure S2 (ESM). The MS^2 spectrum of 2F-QMPSB (Figure 1/ Table S1) with the protonated PI at *m/z* 447.1185 ($C_{22}H_{21}F_2N_2O_4S$) is comparable to data from a previous publication (6). The most abundant fragment ion (FI) is caused by the benzoyl ion at *m/z* 302.0657 ($C_{13}H_{14}F_2NO_3S$) after cleavage of the ester bond. Further cleavage of the piperidine ring leads to the FI at *m/z* 183.0110 ($C_8H_7O_3S$). Following losses of SO_2 and CO results in the FI at *m/z* 119.0491 (C_8H_7O) and *m/z* 91.0542 (C_7H_7). Metabolite QM5 (Figure 1/ Table S1) is the carboxylic acid product after ester hydrolysis with the protonated PI at *m/z* 318.0617 ($C_{13}H_{14}F_2NO_4S$). Loss of CO_2 leads to the FI at *m/z* 274.0719 ($C_{12}H_{14}F_2NO_2S$), followed by loss of HF or 4-methylbenzoate represented by the FIs at *m/z* 254.0657 ($C_{12}H_{13}FNO_2S$) and *m/z* 184.0249 ($C_5H_8F_2NO_2S$).

The HRMS/MS analysis of all incubation mixtures was also carried out in the negative ionization mode, given that earlier studies with the non-fluorinated cannabinoid QMPSB have shown that the carboxylic acid product after ester hydrolysis and the metabolites derived from it could not be detected in the positive ionization mode (11). In fact, all 2F-QMPSB

metabolites which derived from the carboxylic acid part following ester hydrolysis (QM5-QM9; Table S1), could only be detected in the negative ionization mode. Furthermore, the glucuronide and sulfate of 8-hydroxyquinoline (QM12 and QM13; Table S1) could be found in both positive and negative ionization modes, allowing the results from positive ionization mode to be double-checked with the results from the negative ionization mode. Thus, the use of the negative ionization mode in addition to the positive ionization mode can increase the detectability of 2F-QMPSB metabolites and is therefore recommended for the development of bioanalytical screening strategies.

Identification of in vitro phase I and II metabolites of SGT-233

Eight phase I and two phase II metabolites of SGT-233 were tentatively identified in pHLS9 and/or CYP isozyme incubations (metabolites SM1-SM10; Table S2 in the Electronic Supplementary Material, ESM). Table S2 (ESM) depicts the ionization mode (positive or negative) and the incubation type (pHLS9 and/or CYP isozyme incubation) in which the metabolites were detected.

Eight metabolites of SGT-233 were identified in pHLS9 incubations. In contrast to 2F-QMPSB, which shows ester hydrolysis as an important metabolic step, SGT-233 has an amide group instead of an ester group. This amide group was not cleaved under the incubation conditions, so that the cumyl head group is present in all identified metabolites. All metabolites were detected in the one hour as well as in the six hours samples, except for SM3 (*N,N*-bisdealkyl + hydroxy), which could only be detected in the six hours samples.

The MS^2 spectra of SGT-233 and its most abundant metabolite in pHLS9 incubations, the dihydroxy metabolite SM7, are given in Figure 1. MS^2 spectra of further metabolites are given in Figure S3 (ESM). The MS^2 spectrum of SGT-233 (Figure 1/ Table S2) with the

protonated PI at *m/z* 437.1705 ($C_{22}H_{27}F_2N_2O_3S$) is comparable to already published data (6). The loss of the cumyl head group produces the FI at *m/z* 319.0922 ($C_{13}H_{17}F_2N_2O_3S$). Further cleavage of HF and a C4 chain from the piperidine ring leads to the FI at *m/z* 299.0860 ($C_{13}H_{16}FN_2O_3S$) and *m/z* 227.0485 ($C_9H_{11}N_2O_3S$). The FI at *m/z* 134.0600 (C_8H_8NO) is the 4-methylbenzamide core structure and the FI at *m/z* 119.0855 (C_9H_{11}) is the cumyl head group. Further fragmentation of the head group leads to the FI at *m/z* 91.0542 (C_7H_7). The dihydroxy metabolite SM7 (Figure 1/ Table S2) with the PI at *m/z* 469.1603 ($C_{22}H_{27}F_2N_2O_5S$) bears one hydroxy group on the piperidine ring and one on the 4-methyl benzamide core. By losing the cumyl head group, the FI at *m/z* 351.0821 ($C_{13}H_{17}F_2N_2O_5S$) is obtained, which has two more oxygen atoms compared to FI at *m/z* 319.0922 ($C_{13}H_{17}F_2N_2O_3S$) of the parent substance due to dihydroxylation. Further cleavage of the piperidine ring leads to FI at *m/z* 152.0706 ($C_8H_{10}NO_2$) which, in addition to the oxygen of the amide group, also contains a further oxygen atom due to the hydroxylation on the core structure. The two cumyl FIs at *m/z* 119.0855 (C_9H_{11}) and *m/z* 91.0542 (C_7H_7) are unchanged from the parent substance spectrum, which suggested that no hydroxylation took place on the cumyl head group.

In contrast to 2F-QMPSB and its metabolites, SGT-233 and all of its metabolites can be detected in the positive ionization mode. Only the product of sulfonamide cleavage SM2 could also be found with a similar abundance in the negative ionization mode. Therefore, the additional use of the negative ionization mode plays a less important role with SGT-233.

Proposed metabolic pathways of 2F-QMPSB

The proposed metabolic pathways of 2F-QMPSB are depicted in Figure 2. In the in vitro metabolism of 2F-QMPSB, ester hydrolysis is an important step. Therefore, the metabolites were divided into three groups: metabolites with an intact ester group (QM1-QM4), the

carboxylic acid product after ester hydrolysis with additional metabolic reactions (QM5-QM9), and the ester hydrolysis product 8-hydroxyquinoline with additional metabolic reactions (QM10-QM14).

Some phase I metabolites could only be detected in the CYP isozyme incubations and not in the pHLS9 incubations: this was the case for all metabolites with intact ester bonds (QM1-QM4) and the metabolites QM6 and QM11. The reason for this may be that, compared to the CYP incubations, pHLS9 incubations contain human carboxylesterases and the incubation times of the pHLS9 incubations are longer compared to CYP isozyme incubations, which may have resulted in increased ester hydrolysis. Additionally, phase I metabolites can be further metabolized into phase II metabolites in the pHLS9 incubations, whereby the concentration of phase I metabolites could fall under the detection limit. Therefore, it is expected that the metabolites detected in the pHLS9 incubations may be more relevant in vivo compared to the additional phase I metabolites found only in the CYP incubations. Previous in vitro studies on the related SCRAs QMPSB and QMPCB also revealed that no metabolites with an intact ester bond were detectable in the pHLS9 incubations (11). For the SCRA FUB-PB-22, which also has a quinolin-8-yl head group but an *N*-alkyl-1*H*-indole core, no metabolites with an intact ester group were found in an authentic urine sample (17).

Starting from the carboxylic acid product after ester hydrolysis, QM5, hydroxylation of 4-methylbenzoate led to metabolite QM7. Two hydroxylations on the piperidine ring resulted in metabolite QM8. The positions of the hydroxy groups cannot be determined exactly from the fragmentation patterns but can be narrowed down to certain parts of the molecules, such as the core structure in the case of QM7 or the piperidine ring in the case of QM8. In the case of QM8, hydroxylation at the α-position to the nitrogen atom of the piperidine ring is possible, which could lead to ring-opening. This mechanism has already been shown in other substances (18, 19). Further metabolic steps could also lead to the cleavage of the C5 alkyl

chain of piperidine (*N,N*-bisdealkylation), which forms metabolite QM6. QM9 is the acyl glucuronide of the carboxylic acid product QM5. Acyl glucuronides are described in the literature as unstable compounds that tend to hydrolysis and intramolecular acyl migration (20). In fact, the chromatogram with the mass of QM9 indicates several signals that are not baseline separated and are probably caused by the different isomeric acyl glucuronides after acyl migration. However, the putative isomers of the acyl migration show the same MS^2 spectrum. In the case of spontaneous hydrolysis of the acyl glucuronide, the aglycon QM5 is formed accordingly, so that evidence of substance consumption via the aglycon QM5 and other metabolites should still be possible.

8-Hydroxyquinoline (QM10) was hydroxylated in phase I (QM11), although here the position of the hydroxy group could not be determined. Glucuronidation of 8-hydroxyquinoline (QM10) and its hydroxy metabolite QM11 led to the phase II metabolites QM13 and QM14. Sulfation of 8-hydroxyquinoline could also be detected (QM12).

Some metabolites with an intact ester group could be identified (QM1-4). QM3 and QM4 are monohydroxy isomers of 2F-QMPSB which show the same fragmentation pattern but slightly different retention times (Table S1), which would be consistent with different hydroxylation positions at the quinoline head group. QM1 and QM2 result from *N,N*-bisdealkylation of the piperidine ring and a subsequent hydroxylation on the 4-methyl benzoate core.

Brandt et al. have already described two monofluoric impurities contained in the 2F-QMPSB sample, which was also used for these incubations (6). The chemical structures of the impurities are given in Figure S4 (ESM). It is therefore important to mention that the N,N-bisdealkyl metabolite QM1 and the ester hydrolysis product QM10 with metabolites QM2, QM6 and QM11-QM14 derived therefrom can also be metabolites of these two impurities. However, in the carboxylesterases activity assay (see later section) ester hydrolysis of 2F-QMPSB could be identified, which indicates that QM10 and derived metabolites QM11-

QM14 are metabolites originating from 2F-QMPSB. Furthermore, the impurities showed a lower abundance than 2F-QMPSB in the sample (6) and are structurally very similar to 2F-QMPSB. Hence it can also be assumed that the N,N-bisdealkyl metabolites QM1, QM2 and QM6 are metabolites of 2F-QMPSB.

When comparing the detected metabolites of 2F-QMPSB with previous in vitro incubations with the related non-fluorinated SCRA QMPSB (11), it is noticeable that many similar metabolites were identified. The proposed structural formulas for the metabolites QM1, QM6, and QM10 to QM13 were also detected in QMPSB incubations since these do not contain the piperidine ring substituted with fluorine atoms. For the metabolites QM3/QM4, QM5, QM6, QM8, and QM9 which contain the fluorinated piperidine ring, the analogous non-fluorinated structures could be found in the QMPSB incubations. Similar results between the incubations of 2F-QMPSB and QMPSB could be expected due to the very similar structure. However, further metabolites could be detected in QMPSB, in particular metabolites including further metabolic steps on the piperidine ring since QMPSB does not contain any fluorine substituents.

In pHLS9 incubations, the most abundant signals came from the ester hydrolysis products QM5 and QM10 as well as their glucuronides QM9 and QM13 and the glucuronidated monohydroxy metabolite QM14. Therefore, these metabolites are considered as main targets for toxicological screenings. In authentic urine samples after consumption of the related SCRA FUB-PB-22, which also has a quinolin-8-yl head group, the acyl glucuronide of the ester cleavage product was identified as the main metabolite. This could indicate that the acyl glucuronide QM9 is also an important in vivo target for 2F-QMPSB (17). However, it is important to mention that other SCRAs have a 8-hydroxyquinoline ester head group as well, so that 8-hydroxyquinoline and metabolites derived from it are not specific metabolites of 2F-QMPSB though its detection can point to a group of SCARs with this particular head group.

Proposed metabolic pathways of SGT-233

The proposed metabolic pathways of SGT-233 are depicted in Figure 3. In contrast to 2F-QMPSB, SGT-233 has an amide group instead of an ester group, which was not cleaved under the incubation conditions. However, similar metabolic steps as in 2F-QMPSB metabolism could be found such as *N,N*-bisdealkylation (SM1). Derived from SM1, the monohydroxy metabolite SM3 and the dihydroxy metabolite SM4 could be detected. The positions of the hydroxy groups could not be determined accurately based on fragmentation patterns but narrowed down to certain parts of the molecules, like the core structure (SM3) or the cumyl head group (SM4). Metabolite SM2 arises from sulfonamide cleavage. Two monohydroxy metabolites were identified: SM5 is hydroxylated at the cumyl residue and SM6 at the piperidine ring. A further hydroxylation of SM6 on the core structure leads to the dihydroxy metabolite SM7. A trihydroxy metabolite could also be identified (SM8). In phase II metabolism, two glucuronides could be identified: SM9 is the glucuronide of the monohydroxy metabolite SM6 and SM10 the glucuronide of dihydroxy metabolite SM7.

Brandt et al. have also described a monofluoric impurity contained in the SGT-233 sample, which was also used for these incubations (6). The chemical structure of the impurity is depicted in Figure S5 (ESM). Therefore, the *N,N*-bisdealkyl metabolite SM1 with the metabolites SM3 and SM4 derived therefrom and the metabolite SM2 can also be metabolites of this impurity. However, due to the low abundance of the impurity compared to SGT-233 in the samples (6), it is unlikely that these metabolites are only metabolites of the impurity, so they are considered as metabolites of SGT-233.

In pHLS9 incubations, the *N,N*-bisdealkyl metabolite SM1, the hydroxy metabolites SM5, SM7, and SM8, and the glucuronide SM9 had the most abundant signals (Figure 3). Therefore, these metabolites are considered as main targets for toxicological screenings.

Monooxygenases activity screening

The monooxygenases activity screening showed that several monooxygenases are involved in the phase I metabolism of 2F-QMPSB and SGT-233 (Table S3 and S4 in the ESM). Both SCRA were metabolized by CYP2C8, CYP2C9, CYP2C19, CYP3A4, and CYP3A5. In the case of 2F-QMPSB, CYP1A2 was also involved in the metabolism. If a single CYP isoform is inhibited by another substance, the SCRA can thus continue to be degraded via the other CYP isoforms involved. Therefore, a significant change in the hepatic clearance of both SCRA due to a drug-drug interaction causing the inhibition of a single CYP isozyme is unlikely.

Carboxylesterases activity screening of 2F-QMPSB

2F-QMPSB carries a quinolin-8-yl ester head group which has shown rapid ester hydrolysis under the pHLS9 incubation conditions. The instability of this head group is also described in the literature in the form of hydrolysis (5) and transesterification with solvents like methanol or ethanol (21). Hence an carboxylesterases activity screening was carried out for 2F-QMPSB to examine the involvement of different human carboxylesterases in its metabolism. In comparison to 2F-QMPSB, SGT-233 has an amide group instead of the ester group, which was not cleaved under pHLS9 incubation conditions. Therefore, it is assumed that amide cleavage does not play an important role in the metabolism of SGT-233, so no carboxylesterases activity screening was performed for this substance.

Human carboxylesterases catalyze the hydrolysis of many ester-containing endogenous and exogenous substances (14, 22, 23). Previous studies have demonstrated the involvement of hCES1 and hCES2 in the hydrolysis of ester-containing drugs, with hCES1b and hCES1c isoforms being expressed primarily in the liver and hCES2 in the gastrointestinal tract (22, 23). Therefore, 2F-QMPSB was incubated with the recombinant isoforms of hCES1b, hCES1c and hCES2, but also with pHLM and pHLS9, which reflect the presence of natural carboxylesterases in the human liver. However, previous studies with the related SCRA QMPSB have shown that additionally, non-enzymatic ester hydrolysis plays an important role in the degradation of QMPSB (11). To observe possible non-enzymatic hydrolysis, negative control incubations without any enzyme were carried out.

To monitor ester hydrolysis, the carboxylic acid product of ester hydrolysis (metabolite QM5 in Figure 2) was measured. Samples were drawn at multiple time points during the 45 minutes incubation period. The peak area of the carboxylic acid product was normalized to the peak area of the internal standard (glibenclamide) and the value of the 0 min sample was subtracted from the other samples to exclude possible ester hydrolysis before the incubation period. The mean values from duplicate determinations are shown in Figure S6 (ESM). Control incubations of 2F-QMPSB revealed a slight increase in the carboxylic acid product QM5. Since the control incubations did not contain any enzymes, this increase must be the result of non-enzymatic ester hydrolysis. All three human carboxylesterases showed a faster increase of the ester hydrolysis product than the control sample, which suggested enzymatic ester hydrolysis takes place. It was found that the ester hydrolysis product QM5 increases faster with hCES1c and hCES1b compared to hCES2 (Figure S6). Thus, the ester group of 2F-QMPSB seems to be hydrolysed predominantly by hCES1 isoforms. The observation of non-enzymatic ester hydrolysis and additionally enzymatic ester hydrolysis by all three tested hCES isoforms are in agreement with the results of previous in vitro studies with the related

SCRAs QMPSB and QMPCB, which also have a quinolin-8-yl head group (11). The incubations with pHLM and pHLS9 also showed a greater increase in the carboxylic acid ester hydrolysis product compared to the control incubation, so that enzymatic ester hydrolysis must take place here. In both incubations, the parent substance was almost completely degraded after 8 or 14 minutes, so that no further ester hydrolysis could take place. Since the manufacturer does not specify the hCES activities of the pHLM and pHLS9 solutions used, only a qualitative statement can be made here that the natural hCES spectrum in human liver cleaves the ester of 2F-QMPSB.

The carboxylesterases activity screening underlines the importance of ester hydrolysis in the phase I metabolism of 2F-QMPSB. Also, non-enzymatic ester hydrolysis leads to the degradation of 2F-QMPSB, which must be taken into account when processing samples. Therefore, no solvents that can lead to hydrolysis or transesterification should be used in the extraction process or for the storage of stock solutions.

Conclusions

Fourteen metabolites of 2F-QMPSB and ten metabolites of SGT-233 were tentatively identified by LC-HRMS/MS after in vitro incubations. The carboxylesterases activity screening has shown that the ester hydrolysis of 2F-QMPSB is mainly catalyzed by human carboxylesterases 1 isoforms, although non-enzymatic ester hydrolysis had been observed as well. For 2F-QMPSB, it is expected that the ester hydrolysis products and their glucoronides are the most important targets for toxicological plasma and urine screenings. The carboxylic acid part after ester hydrolysis and all metabolites derived from it could only be detected after negative ESI ionization so that the additional use of the negative ionization mode is recommended. For SGT-233, which has an amide linker instead of an ester linker, a cleavage

was not observed under the incubation conditions. Instead, the *N,N*-bisdealkyl metabolite, hydroxy metabolites, and a glucuronide are recommended as targets for toxicological plasma and urine screenings. Monooxygenases activity screening revealed the involvement of several CYP isoforms in the phase I metabolism of both SCRA, mainly CYP2C8, CYP2C9, CYP2C19, CYP3A4, and CYP3A5. Drug-drug interactions regarding the inhibition of a single CYP enzyme are therefore unlikely to have a significant effect on the hepatic clearance of 2F-QMPSB and SGT-233.

Funding

This research received no external funding.

Acknowledgements

The authors like to thank Tanja M. Gampfer, Selina Hemmer, Cathy M. Jacobs, Aline C. Vollmer, Gabriele Ulrich, Thomas P. Bambauer, Matt Bowden, Fabian Frankenfeld, Sascha K. Manier, Wahe G. Okhanian-Saki, Philip Schippers, Carsten Schröder, and Armin A. Weber for their support and/or helpful discussion.

Data Availability Statement

The data underlying this article are available in the article and in its online supplementary material.

Ethics

The current work has been presented at the 58th International Association of Forensic Toxicologists Annual Meeting (TIAFT) 2022.

References

1. (2021) Current NPS threats volume IV, 2021. United Nations Office on Drugs and Crime (UNODC). https://www.unodc.org/documents/scientific/NPS_threats_IV_web.pdf (accessed 17th January 2022).
2. (2021) European Drug Report (EDR) 2021: Trends and Developments. European Monitoring Centre for Drugs and Drug Addiction (EMCDDA). https://www.emcdda.europa.eu/system/files/publications/13838/TDAT21001ENN.pdf (accessed January 17, 2022).
3. (2017) Perspectives on drugs, Synthetic cannabinoids in Europe. Update 6, 2017. European Monitoring Centre for Drugs and Drug Addiction (EMCDDA). https://www.emcdda.europa.eu/system/files/publications/2753/POD_Synthetic%20cannabinoids_0.pdf (accessed January 17, 2022).
4. Lambeng, N., Lebon, F., Christophe, B., Burton, M., De Ryck, M. and Quere, L. (2007) Arylsulfonamides as a new class of cannabinoid CB1 receptor ligands: identification of a lead and initial SAR studies. Bioorganic & Medicinal Chemistry Letters, 17, 272-7.
5. Ermann, M., Riether, D., Walker, E.R., Mushi, I.F., Jenkins, J.E., Noya-Marino, B., et al. (2008) Arylsulfonamide CB2 receptor agonists: SAR and optimization of CB2 selectivity. Bioorganic & Medicinal Chemistry Letters, 18, 1725-9.
6. Brandt, S.D., Kavanagh, P.V., Westphal, F., Dreiseitel, W., Dowling, G., Bowden, M.J., et al. (2021) Synthetic cannabinoid receptor agonists: Analytical profiles and development of QMPSB, QMMSB, QMPCB, 2F-QMPSB, QMiPSB, and SGT-233. Drug Testing and Analysis, 13, 175-196.
7. Tsochatzis, E.D., Alberto Lopes, J., Holland, M.V., Reniero, F., Palmieri, G. and Guillou, C. (2021) Identification and analytical characterization of a novel synthetic cannabinoid-type substance in herbal material in Europe. Molecules, 26.
8. Uchiyama, N., Matsuda, S., Kawamura, M., Kikura-Hanajiri, R. and Goda, Y. (2013) Two new-type cannabimimetic quinolinyl carboxylates, QUPIC and QUCHIC, two new cannabimimetic carboxamide derivatives, ADB-FUBINACA and ADBICA, and five synthetic cannabinoids detected with a thiophene derivative α-PVT and an opioid receptor agonist AH-7921 identified in illegal products. Forensic Toxicol, 31, 223-240.
9. Staeheli, S.N., Poetzsch, M., Veloso, V.P., Bovens, M., Bissig, C., Steuer, A.E., et al. (2018) In vitro metabolism of the synthetic cannabinoids CUMYL-PINACA, 5F-CUMYL-PINACA, CUMYL-4CN-BINACA, 5F-CUMYL-P7AICA and CUMYL-4CN-B7AICA. Drug Testing and Analysis, 10, 148-157.
10. Wagmann, L. and Maurer, H.H. (2018) Bioanalytical methods for new psychoactive substances. Handbook of Experimental Pharmacology, 252, 413-439.
11. Richter, M.J., Wagmann, L., Gampfer, T.M., Brandt, S.D. and Meyer, M.R. (2021) In vitro metabolic fate of the synthetic cannabinoid receptor agonists QMPSB and QMPCB (SGT-11) including isozyme mapping and esterase activity. Metabolites, 11.
12. Richter, L.H.J., Flockerzi, V., Maurer, H.H. and Meyer, M.R. (2017) Pooled human liver preparations, HepaRG, or HepG2 cell lines for metabolism studies of new psychoactive substances? A study using MDMA, MDBD, butylone, MDPPP, MDPV, MDPB, 5-MAPB, and 5-API as examples. Journal of Pharmaceutical and Biomedical Analysis, 143, 32-42.
13. Wagmann, L., Meyer, M.R. and Maurer, H.H. (2016) What is the contribution of human FMO3 in the N-oxygenation of selected therapeutic drugs and drugs of abuse? Toxicol Lett, 258, 55-70.
14. Meyer, M.R., Schutz, A. and Maurer, H.H. (2015) Contribution of human esterases to the metabolism of selected drugs of abuse. Toxicology Letters, 232, 159-66.
15. Helfer, A.G., Michely, J.A., Weber, A.A., Meyer, M.R. and Maurer, H.H. (2015) Orbitrap technology for comprehensive metabolite-based liquid chromatographic-high resolution-

tandem mass spectrometric urine drug screening - exemplified for cardiovascular drugs. Anal Chim Acta, 891, 221-33.
16. Wagmann, L., Manier, S.K., Felske, C., Gampfer, T.M., Richter, M.J., Eckstein, N., et al. (2021) Flubromazolam-Derived Designer Benzodiazepines: Toxicokinetics and Analytical Toxicology of Clobromazolam and Bromazolam. Journal of Analytical Toxicology, 45, 1014-1027.
17. Diao, X., Scheidweiler, K.B., Wohlfarth, A., Pang, S., Kronstrand, R. and Huestis, M.A. (2016) In vitro and in vivo human metabolism of synthetic cannabinoids FDU-PB-22 and FUB-PB-22. The AAPS Journal, 18, 455-64.
18. Holsztynska, E.J. and Domino, E.F. (1985) Biotransformation of phencyclidine. Drug Metabolism Reviews, 16, 285-320.
19. JA, A.M., Manier, S.K., Caspar, A.T., Brandt, S.D., Wallach, J. and Maurer, H.H. (2017) New psychoactive substances 3-Methoxyphencyclidine (3-MeO-PCP) and 3-Methoxyrolicyclidine (3-MeO-PCPy): metabolic fate elucidated with rat urine and human liver preparations and their detectability in urine by GC-MS, "LC-(High Resolution)-MSn" and "LC-(High Resolution)-MS/MS". Current Neuropharmacology, 15, 692-712.
20. Ebner, T., Heinzel, G., Prox, A., Beschke, K. and Wachsmuth, H. (1999) Disposition and chemical stability of telmisartan 1-O-acylglucuronide. Drug Metabolism and Disposition, 27, 1143-9.
21. Blakey, K., Boyd, S., Atkinson, S., Wolf, J., Slottje, P.M., Goodchild, K., et al. (2016) Identification of the novel synthetic cannabimimetic 8-quinolinyl 4-methyl-3-(1-piperidinylsulfonyl)benzoate (QMPSB) and other designer drugs in herbal incense. Forensic Science International, 260, 40-53.
22. Thomsen, R., Rasmussen, H.B., Linnet, K. and Consortium, I. (2014) In vitro drug metabolism by human carboxylesterase 1: focus on angiotensin-converting enzyme inhibitors. Drug Metabolism and Disposition, 42, 126-33.
23. Wang, J., Williams, E.T., Bourgea, J., Wong, Y.N. and Patten, C.J. (2011) Characterization of recombinant human carboxylesterases: fluorescein diacetate as a probe substrate for human carboxylesterase 2. Drug Metabolism and Disposition, 39, 1329-33.

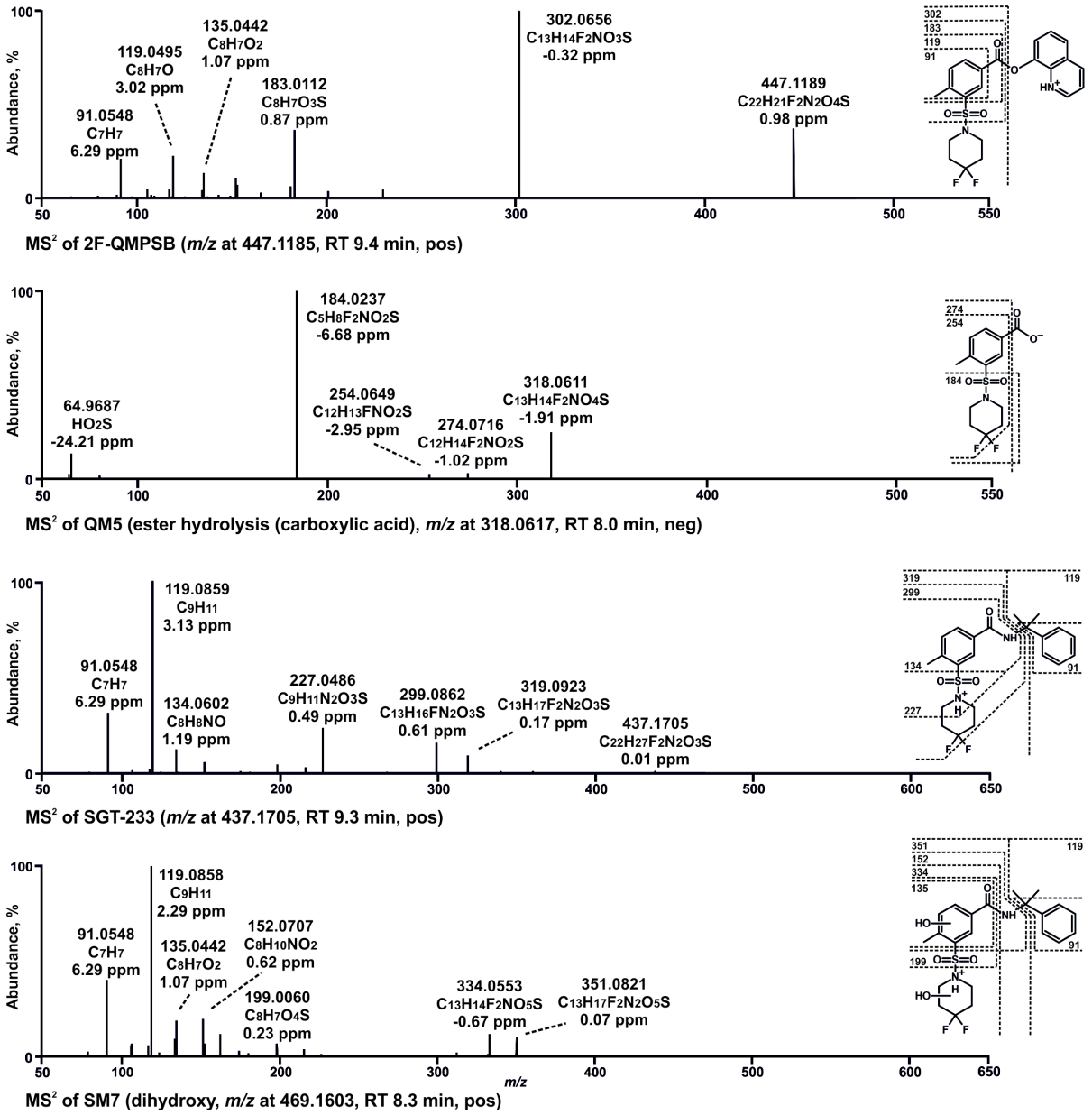

Figure 1. High-resolution MS^2 spectra of 2F-QMPSB and SGT-233 and their most abundant metabolites detected in pooled human liver S9 incubations (QM5 and SM7). RT, retention time; pos, positive ionization mode; neg, negative ionization mode; gluc, glucuronic acid.

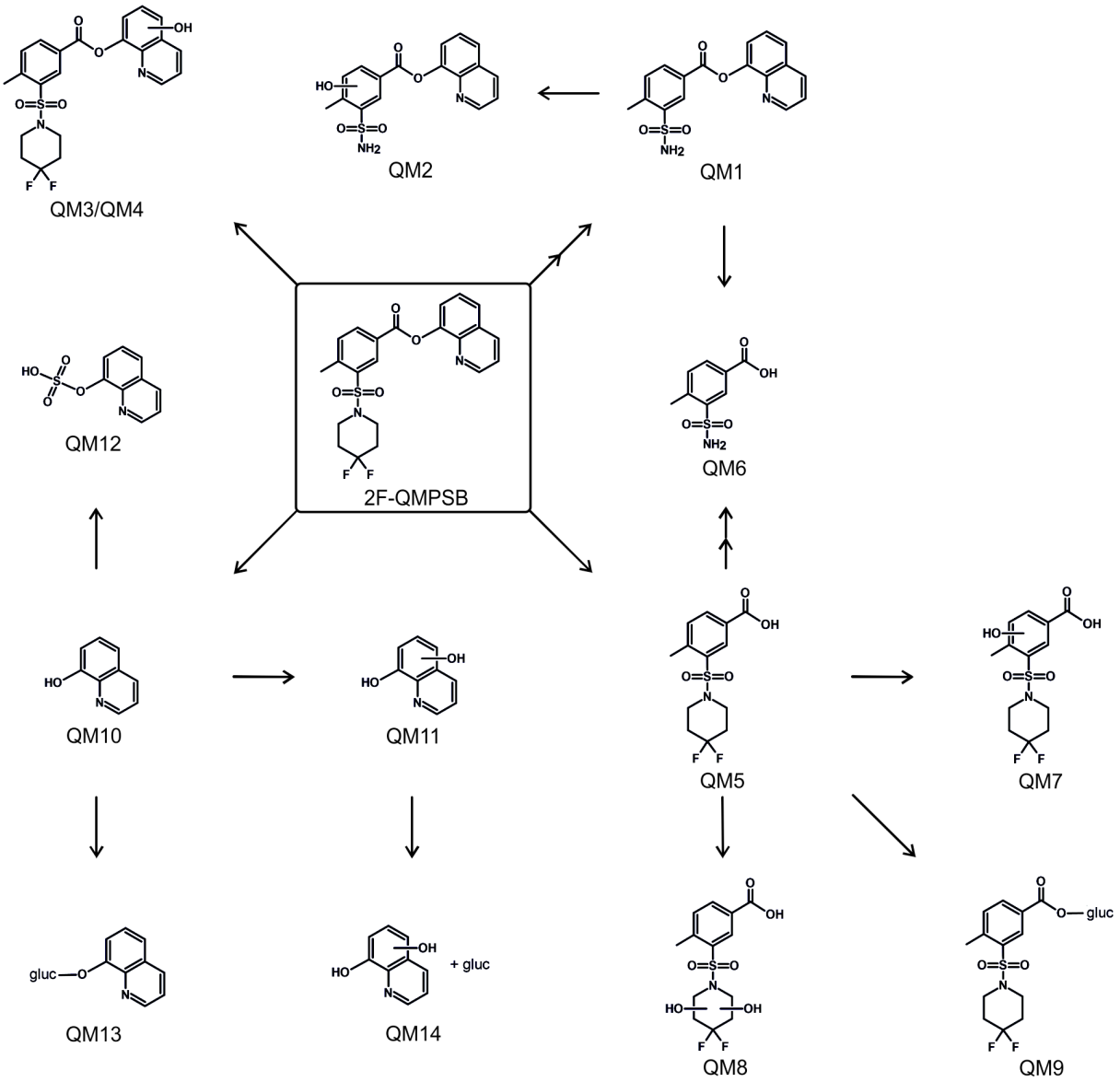

Figure 2. Proposed in vitro metabolic pathways of 2F-QMPSB. QM1-QM14, metabolites of 2F-QMPSB; gluc, glucuronic acid.

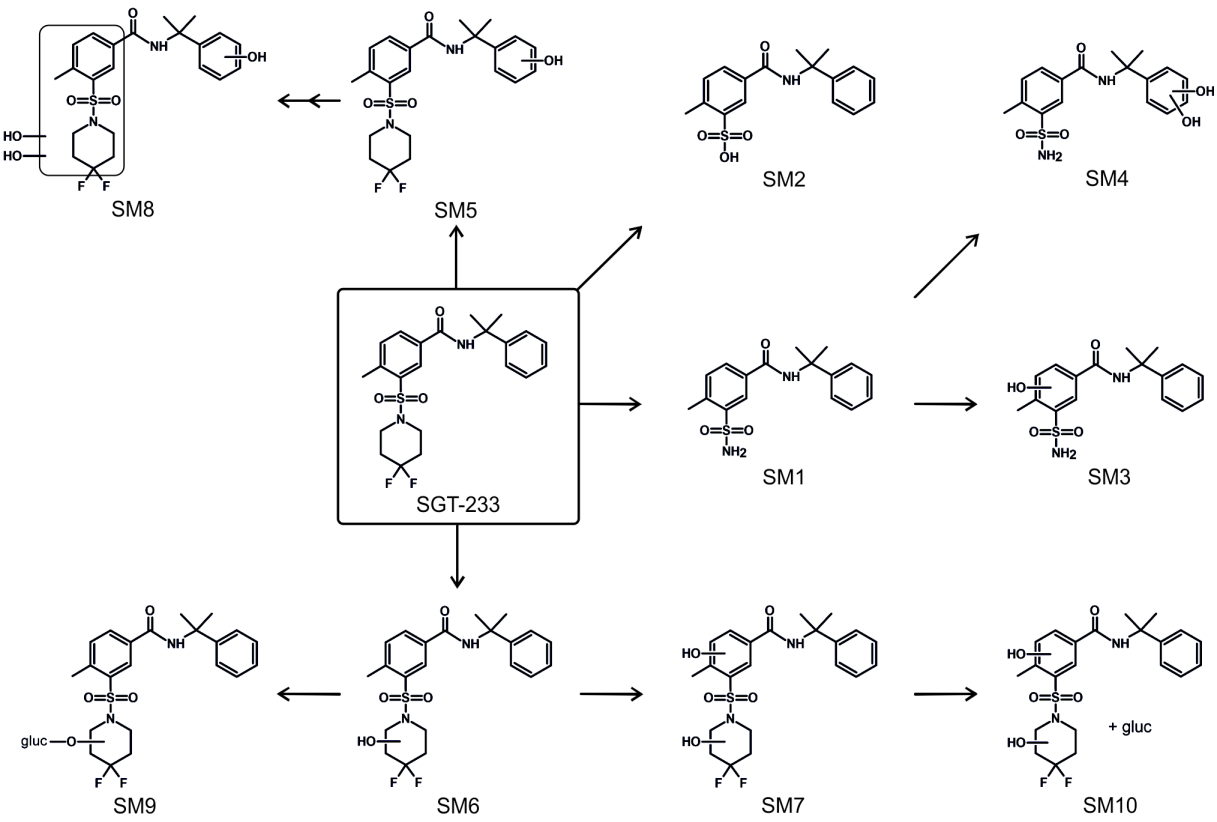

Figure 3. Proposed in vitro metabolic pathways of SGT-233. SM1-SM10, metabolites of SGT-233; gluc, glucuronic acid.